METHODS IN MOLECULAR BIOLOGY

Series Editor
John M. Walker
School of Life and Medical Sciences
University of Hertfordshire
Hatfield, Hertfordshire, AL10 9AB, UK

For further volumes:
http://www.springer.com/series/7651

Adipose-Derived Stem Cells

Methods and Protocols

Second Edition

Edited by

Bruce A. Bunnell

Center for Stem Cell Research and Regenerative Medicine, Tulane University School of Medicine, New Orleans, LA, USA

Jeffrey M. Gimble

Center for Stem Cell Research and Regenerative Medicine, Tulane University School of Medicine, New Orleans, LA, USA; LaCell LLC, New Orleans, LA, USA

Humana Press

Editors
Bruce A. Bunnell
Center for Stem Cell Research and Regenerative Medicine
Tulane University School of Medicine
New Orleans, LA, USA

Jeffrey M. Gimble
Center for Stem Cell Research and Regenerative Medicine
Tulane University School of Medicine
New Orleans, LA, USA

LaCell LLC
New Orleans, LA, USA

ISSN 1064-3745 ISSN 1940-6029 (electronic)
Methods in Molecular Biology
ISBN 978-1-4939-7797-0 ISBN 978-1-4939-7799-4 (eBook)
https://doi.org/10.1007/978-1-4939-7799-4

Library of Congress Control Number: 2018938174

Cover caption: Cover image courtesy of Rachel Sabol.

Printed on acid-free paper

This Humana Press imprint is published by the registered company Springer Science+Business Media, LLC part of Springer Nature.
The registered company address is: 233 Spring Street, New York, NY 10013, U.S.A.

Preface

Adipose stromal/stem cells (ASC) remain of intense interest in the field of regenerative medicine for their potent differentiation, immunomodulatory potential, and paracrine actions via their secretome. Over the intervening time since the publication of the first edition of this book, the use of the stroma vascular fraction (SVF) as a potential therapeutic strategy has gained momentum. The SVF is obtained from processed adipose tissue and is composed of a heterogeneous mesenchymal population of cells that includes not only adipose stromal and hematopoietic stem and progenitor cells but also endothelial cells, erythrocytes, fibroblasts, lymphocytes, monocyte/macrophages, and pericytes. The SVF has been demonstrated to possess both anti-inflammatory and differentiation potential. In this second volume of *Methods in Molecular Biology* focused on ASC and SVF, we have again obtained well-defined and thoroughly vetted protocols from leaders in the field. The chapters are focused on protocols centered around the discovery, preclinical, and clinical processes. Emphasis was placed on human ASC again; however, additional small and large animal species with preclinical relevance are included. Many of the protocols are new to this edition and represent scientific advances in the field of ASC biology and application, while others represent refinements and enhancements in previously published protocols.

The editors have many people to thank for their contributions to this work: First and foremost our colleagues who were kind enough to find time in their busy schedules to author the chapters found in this edition. We would also like to thank Professor John Walker, Series Editor, and the editorial staff at Springer whose direction, advice, and occasional prodding were greatly needed and deeply appreciated. Finally, we would also like to thank our families for permitting us the time required on nights and weekends to complete this work.

New Orleans, LA, USA

Bruce A. Bunnell
Jeffrey M. Gimble

Contents

Contributors

Joel A. Aronowitz · *Cedars-Sinai Medical Center, Los Angeles, CA, USA; University Stem Cell Center, Los Angeles, CA, USA*

Josie C. Bodle · *Joint Department of Biomedical Engineering, North Carolina State University and University of North Carolina Chapel Hill, Raleigh, NC, USA*

Annie C. Bowles · *Department of Cell and Molecular Biology, Tulane University School of Science and Engineering, New Orleans, LA, USA; Center for Stem Cell Research and Regenerative Medicine, Tulane University School of Medicine, New Orleans, LA, USA*

Cody Brown · *Department of Anatomy and Cell Biology, Schulich School of Medicine and Dentistry, The University of Western Ontario, London, ON, Canada*

Bruce A. Bunnell · *Center for Stem Cell Research and Regenerative Medicine, Tulane University School of Medicine, New Orleans, LA, USA; Department of Pharmacology, Tulane University School of Medicine, New Orleans, LA, USA*

Valerio Cervelli · *Department of Plastic and Reconstructive Surgery, University of Rome "Tor Vergata", Rome, Italy*

Rodney K. Chan · *United States Army Institute of Surgical Research, JBSA Fort Sam Houston, TX, USA*

Nicholas Clark · *Regenerative Medicine Department, Naval Medical Research Center, Silver Spring, MD, USA*

J. Lowry Curley · *Center for Stem Cell Research and Regenerative Medicine, Tulane University School of Medicine, New Orleans, LA, USA; LaCell LLC, New Orleans, LA, USA*

Christian Dani · *Faculté de Médecine, Université Nice Sophia Antipolis, iBV, UMR CNRS/INSERM, Nice Cedex 2, France*

Alexes C. Daquinag · *Brown Foundation Institute of Molecular Medicine for the Prevention of Human Diseases, University of Texas Health Science Center at Houston, Houston, TX, USA*

Thomas A. Davis · *Regenerative Medicine Department, Naval Medical Research Center, Silver Spring, MD, USA; Department of Surgery, Uniformed Services University of the Health Sciences, Bethesda, MD, USA*

Ram Devireddy · *Bioengineering Laboratory, Department of Mechanical Engineering, Louisiana State University, Baton Rouge, LA, USA*

Marilyn Dietrich · *Pennington Biomedical Research Center, Louisiana State University System, Baton Rouge, LA, USA*

Wei Duan · *Laboratory for Equine and Comparative Orthopedic Research, School of Veterinary Medicine, Louisiana State University, Baton Rouge, LA, USA*

Francesco Egro · *University of Pittsburgh, Pittsburgh, PA, USA*

Margo Emont · *Life Sciences Institute, University of Michigan, Ann Arbor, MI, USA; Department of Molecular and Integrative Physiology, University of Michigan, Ann Arbor, MI, USA*

Carmel Fargason · *Laboratory for Equine and Comparative Orthopedic Research, School of Veterinary Medicine, Louisiana State University, Baton Rouge, LA, USA*

Z. Elizabeth Floyd · *Ubiquitin Laboratory, Pennington Biomedical Research Center, Louisiana State University System, Baton Rouge, LA, USA*

Lauren E. Flynn · *Department of Anatomy and Cell Biology, Schulich School of Medicine and Dentistry, The University of Western Ontario, London, ON, Canada; Department of Chemical and Biochemical Engineering, Thompson Engineering Building, The University of Western Ontario, London, ON, Canada; Department of Chemical Engineering, Queen's University, Kingston, ON, Canada*

Anoosha Forghani · *Bioengineering Laboratory, Department of Mechanical Engineering, Louisiana State University, Baton Rouge, LA, USA*

Anthony D. Foster · *Regenerative Medicine Department, Naval Medical Research Center, Silver Spring, MD, USA; Department of Surgery, Uniformed Services University of the Health Sciences, Bethesda, MD, USA*

Julie Fradette · *Centre de Recherche en Organogénèse Expérimentale de l'Université Laval/LOEX, CRCHU de Québec-Université Laval, Québec, QC, Canada; Department of Surgery, Faculty of Medicine, Université Laval, Québec, QC, Canada; CMDGT/LOEX, Aile–R, Pavilion Hôpital Enfant-Jésus, CRCHU de Québec-Université Laval, Québec, QC, Canada*

Pietro Gentile · *Department of Plastic and Reconstructive Surgery, University of Rome "Tor Vergata", Rome, Italy; Catholic University, Tirane, Albania*

Jeffrey M. Gimble · *Center for Stem Cell Research and Regenerative Medicine, Tulane University School of Medicine, New Orleans, LA, USA; LaCell LLC, New Orleans, LA, USA*

Warren L. Grayson · *Department of Biomedical Engineering, Johns Hopkins University School of Medicine, Baltimore, MD, USA; Translational Tissue Engineering Center, Johns Hopkins University School of Medicine, Baltimore, MD, USA; Department of Materials Science and Engineering, Johns Hopkins University Whiting School of Engineering, Baltimore, MD, USA*

Anne-Laure Hafner · *Faculté de Médecine, Université Nice Sophia Antipolis, iBV, UMR CNRS/INSERM, Nice Cedex 2, France*

Cloe S. Hakakian · *University Stem Cell Center, Los Angeles, CA, USA*

Yuan Di C. Halvorsen · *Center for Computational and Integrative Biology, Harvard Medical School, Boston, MA, USA*

Pinar Yilgor Huri · *Department of Biomedical Engineering, Johns Hopkins University School of Medicine, Baltimore, MD, USA; Translational Tissue Engineering Center, Johns Hopkins University School of Medicine, Baltimore, MD, USA; Department of Biomedical Engineering, Ankara University Faculty of Engineering, Ankara, Turkey*

Heejin Jun · *Life Sciences Institute, University of Michigan, Ann Arbor, MI, USA*

Gail Kilroy · *Pennington Biomedical Research Center, Louisiana State University System, Baton Rouge, LA, USA*

Mikhail G. Kolonin · *Brown Foundation Institute of Molecular Medicine for the Prevention of Human Diseases, University of Texas Health Science Center at Houston, Houston, TX, USA*

Kai P. Leung · *United States Army Institute of Surgical Research, JBSA Fort Sam Houston, TX, USA*

Hui Li · *National Engineering Laboratory for Oral Regenerative Medicine, West China Hospital of Stomatology, Sichuan University, Chengdu, China; Life Sciences Institute, University of Michigan, Ann Arbor, MI, USA*

Jie Li · *Center for Stem Cell Research and Regenerative Medicine, Tulane University School of Medicine, New Orleans, LA, USA; LaCell LLC, New Orleans, LA, USA; National Engineering Laboratory for Oral Regenerative Medicine, West China Hospital of Stomatology, Sichuan University, Chengdu, China*

Elizabeth G. Loboa · *College of Engineering, University of Missouri, Columbia, MO, USA*

Ryan A. Lockhart · *University Stem Cell Center, Los Angeles, CA, USA*

Mandi J. Lopez · *Laboratory for Equine and Comparative Orthopedic Research, School of Veterinary Medicine, Louisiana State University, Baton Rouge, LA, USA*

Kacey G. Marra · *University of Pittsburgh, Pittsburgh, PA, USA*

Pascal Morissette Martin · *Department of Anatomy and Cell Biology, Schulich School of Medicine and Dentistry, The University of Western Ontario, London, ON, Canada*

Dominique Mayrand · *Centre de Recherche en Organogénèse Expérimentale de l'Université Laval/LOEX, CRCHU de Québec-Université Laval, Québec, QC, Canada; Department of Surgery, Faculty of Medicine, Université Laval, Québec, QC, Canada*

Hiroshi Mizuno · *Department of Plastic and Reconstructive Surgery, Juntendo University School of Medicine, Tokyo, Japan*

Tala Mohsen-Kanson · *Faculté de Médecine, Université Nice Sophia Antipolis, iBV, UMR CNRS/INSERM, Nice Cedex 2, France; Department of Biology, Faculty of Sciences II, Lebanese University, Fanar, Lebanon*

Justin Morrissette-McAlmon · *Department of Biomedical Engineering, Johns Hopkins University School of Medicine, Baltimore, MD, USA; Translational Tissue Engineering Center, Johns Hopkins University School of Medicine, Baltimore, MD, USA*

Rachel C. Nordberg · *Joint Department of Biomedical Engineering, North Carolina State University and University of North Carolina Chapel Hill, Raleigh, NC, USA*

Christina L. Rettinger · *United States Army Institute of Surgical Research, JBSA Fort Sam Houston, TX, USA*

Shahensha Shaik · *Bioengineering Laboratory, Department of Mechanical Engineering, Louisiana State University, Baton Rouge, LA, USA*

Arthi Shridhar · *Department of Chemical and Biochemical Engineering, Thompson Engineering Building, The University of Western Ontario, London, ON, Canada*

Glauco R. Souza · *Nano3D Biosciences, Houston, TX, USA; Oncology Division, Department of Internal Medicine, UT Health Science Center at Houston, Houston, TX, USA*

Satoshi Tajima · *Department of Plastic and Reconstructive Surgery, Juntendo University School of Medicine, Tokyo, Japan; Department of Dentistry and Oral Surgery, AOI Universal Hospital, Kanagawa, Japan*

Weidong Tian · *National Engineering Laboratory for Oral Regenerative Medicine, West China Hospital of Stomatology, Sichuan University, Chengdu, China*

Morikuni Tobita · *Department of Plastic and Reconstructive Surgery, Juntendo University School of Medicine, Tokyo, Japan*

Hubert Tseng · *Nano3D Biosciences, Houston, TX, USA*

Alan Tucker · *Center for Stem Cell Research and Regenerative Medicine, Tulane University School of Medicine, New Orleans, LA, USA*

Jun Wu · *Life Sciences Institute, University of Michigan, Ann Arbor, MI, USA; Department of Molecular and Integrative Physiology, University of Michigan, Ann Arbor, MI, USA*
Xiying Wu · *Center for Stem Cell Research and Regenerative Medicine, Tulane University School of Medicine, New Orleans, LA, USA; LaCell LLC, New Orleans, LA, USA*
Claire Yu · *Department of Chemical Engineering, Queen's University, Kingston, ON, Canada*
Hui Yu · *Life Sciences Institute, University of Michigan, Ann Arbor, MI, USA*
Nan Zhang · *Laboratory for Equine and Comparative Orthopedic Research, School of Veterinary Medicine, Louisiana State University, Baton Rouge, LA, USA*

Chapter 1

Isolation and Flow Cytometric Analysis of the Stromal Vascular Fraction Isolated from Mouse Adipose Tissue

Annie C. Bowles, Alan Tucker, and Bruce A. Bunnell

Abstract

Evidence from preclinical research and clinical trials demonstrates the use of the stromal vascular fraction (SVF) as therapy for numerous indications. These results demonstrate that autologous SVF is not only safe and effective but provides robust anti-inflammatory, immunomodulatory, and reparative effects in vivo. The potency of the SVF is attributed to the cellular composition which includes adipose-derived stem cells (ASCs), adipocytes, endothelial cells, and various immune cells. As the name would suggest, these SVF cells are derived from the stromal compartment of adipose, or fat. Once digested, the cells that constitute adipose are released and collected as the SVF. The cellular frequencies within the SVF can then be assessed using a fluorescent antibody-based technique known as flow cytometry. The following chapter provides a standard operating protocol that describes the procedures from harvesting the fat tissue from experimental mice to isolating and characterizing the SVF.

Key words Stromal vascular fraction, Adipose-derived stem cells, Adipose tissue, Flow cytometry, Immunophenotyping

1 Introduction

Fat or adipose is the largest endocrine organ of the body involved in thermoregulation, insulation, cushioning, and energy storage [1, 2]. It is a highly vascularized tissue that is mainly composed of connective tissue and adipocytes, and is an attractive source of stem cells, called adipose-derived stem cells (ASCs) [3, 4]. When fat is collected, digested and centrifuged, three layers are created. The bottom layer, or pellet, is called the stromal vascular fraction (SVF) [4, 5]. This concentrated cellular pellet contains the adipocytes, ASCs, endothelial cells, and numerous types of immune cells [2, 3]. Clinically, human donors of autologous fat can be removed by a minimally invasive liposuction procedure then rapidly digested, processed, and administered back to the patient as SVF during the same procedure [6]. This abundant source of cells has demonstrated

Bruce A. Bunnell and Jeffrey M. Gimble (eds.), *Adipose-Derived Stem Cells: Methods and Protocols*, Methods in Molecular Biology, vol. 1773, https://doi.org/10.1007/978-1-4939-7799-4_1,

potent anti-inflammatory, immunomodulatory, and reparative effects in vivo [7].

In humans, SVF is commonly used to supplement fat grafting in cosmetic and reconstructive surgery and is believed to attenuate the resorption process [6, 8]. Veterinary medicine has demonstrated the safe and effective treatment of bone, tendon, and joint injuries and osteoarthritis in over thousands of large animals [9, 10]. In a murine model of multiple sclerosis, the SVF has demonstrated attenuation of disease, modulation of the inflammatory disease milieu and improvement of motor function [11, 12]. Collectively, this evidence demonstrates the safe and effective use of SVF for treating many medical indications.

This chapter described a widely used method of SVF isolation from murine adipose that yields consistent outcomes and is easily reproduced. The protocol begins with harvesting the inguinal white adipose tissue from mice, and then describes the methods of digestion, isolation, and characterization of the composition of the SVF. Additionally, a comprehensive panel of cellular markers is provided for flow cytometric analysis to determine the frequency of desired cell types within the SVF.

2 Materials

2.1 Animals

1. C57Bl/6 mice.

2.2 Reagents

1. Dulbecco's modified Eagle medium: Ham's F-12 (DMEM/F-12).
2. Fetal bovine serum (FBS), premium select, hybridoma qualified not heat inactivated.
3. L-glutamine (200 mM) in solution of 0.85% NaCl.
4. Antibiotic–antimycotic (anti-anti; 100×).
5. Phosphate buffered saline (PBS) without Ca^{2+} or Mg^{2+}, 1×.
6. Bovine serum albumin (BSA), lyophilized powder, essentially fatty acid free.
7. Collagenase type-I, 390 U/mg.
8. 0.25% trypsin and 1 mM ethylenediaminetetraacetic acid (EDTA) in Hanks' Balanced Salt Solution (HBSS).
9. 0.4% Trypan Blue in solution of 0.85% NaCl.
10. Distilled, deionized water (DDI-H_2O).
11. 4% paraformaldehyde (PFA) in PBS.
12. Fixation/permeabilization concentrate.
13. Fixation/permeabilization diluent.

2.3 Supplies

1. Flow cytometry antibodies (*see* Table 1).
2. 500 ml vacuum-driven filtration unit with 0.22-μm pore size.

Table 1
Anti-mouse antibodies for determining the cell frequencies in the SVF

Antibody	Clone	Isotype	Affinity
CD3	17A2	IgG	All T cells
CD4	GK1.5	IgG2b	Helper T cells, regulatory T cells
CD8	53–6.7	IgG2b	Cytotoxic T cells
CD14	SA2–8	IgG2a	Monocytes/macrophages
CD19	1D3	IgG2a	B cells
CD25	7D4	IgG2a	Regulatory T cells
CD31	390	IgG2a	Endothelial cells, lymphocytes
CD34	RAM34	IgG2a	HSC, dendritic cells
CD36	72-1	IgG2a	Dendritic cells, monocytes/macrophages
CD45	30-F11	IgG2b	All leukocytes
CD68[a]	FA11	IgG2a	Monocytes/macrophages
CD90	HIS51	IgG2a	HSC, MSC, monocytes/macrophages
F4/80	BM8	IgG2a	Dendritic cells, monocytes
FCeR1	MAR-1	IgG	Mast cells
foxp3[a]	FJK-16 s	IgG2a	Regulatory T cells
Ly6G	RB6-8C5	IgG2	Granulocytes
Sca-1	D7	IgG2a	HSC, MSC

HSC hematopoietic stem cells, *MSC* mesenchymal stem cells
[a]Intracellular markers that require fixation and permeabilization protocol

3. Sterile scissors and forceps.
4. Sterile 50 ml polystyrene collection tubes.
5. 50 ml vacuum-driven filtration unit with 0.22-μm pore size.
6. Sterile microcentrifuge tubes.
7. Micropipettes and pipettes with sterile tips.
8. Parafilm.

2.4 Equipment

1. Scale milligram to gram measurements.
2. Biological safety cabinet, class II with vacuum aspiration source with tubing and waste container.
3. Incubator, water jacketed and humidified with 5% CO_2, maintained at 37 °C
4. Inverted phase-contrast microscope.
5. Large and small centrifuges.

6. Rocker incubator.
7. Flow cytometer, with eight-color-capability.
8. Water bath with autoclaved water, maintained at 37 °C.

2.5 Solutions

1. Complete culture media (CCM): Dulbecco's modified Eagle medium: Ham's F-12.

   10% fetal bovine serum.

   1% 2 mM L-glutamine.

   1% antibiotic–antimycotic.
2. Adipose digestion solution (w/v; grams of adipose to milliliters of PBS):

   0.1% collagenase Type I.

   1% BSA.
3. 1% PFA (optional): 4% PFA in DDI-H_2O (1:3).
4. Working fixation/permeabilization solution: fixation/permeabilization concentrate in diluent (1:3).
5. 1× Working Perm. Buffer.

   10× Perm. Buffer in DDI-H_2O (1:10).

3 Methods

3.1 Isolation of the Inguinal White Adipose Tissue

The following procedure is performed after euthanasia of the experimental animals. It is recommended that each animal is secured dorsum down where the ventral surface is accessible for the isolation of white fat tissue from the inguinal area (Fig. 1).

1. Make a small incision beneath the sternum using forceps and surgical scissors.
2. Insert scissors into incision and blunt dissect between the skin and peritoneum forming a pocket.
3. Make a large, vertical incision from the initial incision down to the genitalia area.
4. Make pockets around each flank by securing the skin with forceps and inserting the scissors between the skin and peritoneum followed by blunt dissections.
5. Make a horizontal incision from the initial incision to the back of one side of the mouse.
6. Expose the inguinal fat pad lying between the skin and the peritoneum.
7. Fold the skin inside-out and securely pin the loose corner.

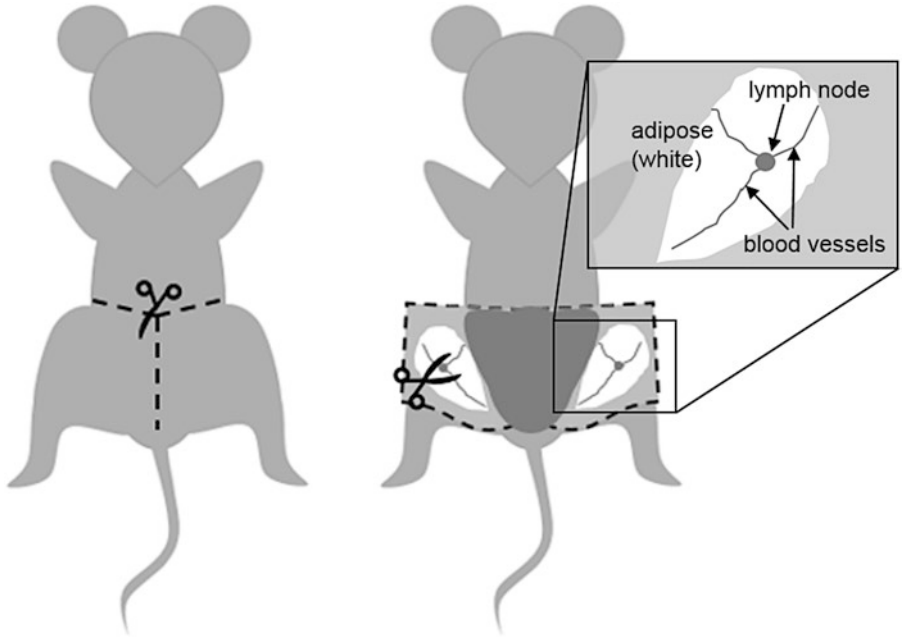

Fig. 1 Isolation of the inguinal white adipose tissue from mice

8. Identify and remove the lymph node located in the middle of the fat pat (*see* **Note 1**).
9. Carefully excise the entire fat pad and collect the fat in a conical tube.
10. Repeat **steps 5–9** for excision of the alternate inguinal fat pad.

3.2 Isolation of the Stromal Vascular Fraction

1. Collect fat tissue in a 50 ml conical tube.
2. Weigh fat.
   Under a biosafety hood:
3. Wash fat by adding ample PBS and vigorously shake the capped conical tube.
4. Transfer fat to a fresh tube.
5. Repeat **steps 3** and **4** until solution is clear.
6. Transfer washed fat to a fresh tube. Put aside conical tube containing fat tissue.
7. In a fresh 50 ml conical tube, make digestion solution.
8. Gently rock conical tube to dissolve solutes; do not vortex.
9. Secure the 50 ml disposable vacuum filtration system with 0.22-μm pore size to conical tube with digestion solution.
10. Attach vacuum tubing to filter unit and vacuum port.

11. Filter digestion solution into attached collection tube.
12. Add filtered digestion solution to tube containing the fat tissue.
13. Start a timer for 1 h.
14. Quickly mince fat in digestion solution with scissors by downward motion cutting in the tube (*see* **Note 2**).
15. Add Parafilm around top of tube to seal.
16. Place tube with fat tissue in digestion solution into an incubator shaker.
17. Incubate fat in digestion solution at 37 °C in incubator for time remaining. Set shaker speed to 100 rpm.

Proceed under a biological safety cabinet henceforth.

18. Prepare 500 ml CCM.
19. Using the 500 ml vacuum-driven filtration unit with 0.22-μm pore size, filter CCM into the collection reservoir.
20. Warm CCM in water bath at 37 °C (*see* **Note 3**).
21. After 1 h incubation of fat in the digestion solution, remove tube from incubator shaker and return under biosafety hood.
22. Neutralize digestion solution by adding (v/v) CCM to the tube.
23. Cap the tube and invert several times to mix.
24. Centrifuge conical tube for 5 min at 500 ×*g* at room temperature (RT).
25. Remove and shake conical tube to assist in the release of cells from tissue.
26. Centrifuge conical tube again for 5 min at 500 ×*g* at RT.
27. Carefully remove conical tube from centrifuge. Be sure not to disturb layers.
28. Carefully aspirate top liquid layers leaving pellet of stromal vascular fraction (SVF).
29. Add CCM to conical tube to resuspend cells of SVF by pipetting up and down several times.
30. Filter cell suspension through sterile gauze to remove any hair or large debris and collect in a fresh 50 ml conical tube.
31. Count live cells using Trypan Blue exclusion method and determine total live cell count.

Solution now consists of a single-cell suspension of SVF cells. Cells can be prepared in a saline solution for experimental use or analyzed by flow cytometric analysis as described below.

3.3 Staining Cells for Flow Cytometric Analysis

1. Determine the concentration of live SVF cells in known volume of PBS.
2. Aliquot between 2.5×10^5 and 5×10^5 cells in approximately 100 µl per microcentrifuge tube for each protocol (Table 2; *see* **Note 4**).
3. Stain cells in each microcentrifuge tube by pipetting 1–5 µl of each antibody in each panel according to Table 2. Initial titration of antibodies will determine appropriate volume of antibody used per sample. (Additional antibody for live/dead staining is optional).
4. Cap and vortex tubes for 5 s.
5. Incubate tubes for 15 min at RT in the dark.
6. Wash by adding 1.0–1.5 ml of PBS to each tube.
7. Centrifuge tubes at 500 ×*g* for 5 min.
8. Decant by quickly inverting tube once over a waste beaker. This should allow approximately 100 µl to remain over the cell pellet.
9. (Optional) Repeat **steps 6–11** for secondary antibodies.
10. Wash again by repeating **steps 9–11**.

Table 2
Sample panel for analysis of the frequencies of subpopulations within the SVF

Panel	Antibody–fluorochrome
Protocol 1 Requires fixation and permeabilization[a]	CD4–PE CD3–PE610 CDCD8–PeCy5 foxp3–APC[a]
Protocol 2	CD19–PE610 FCεRI–PeCy7 CD45–APC
Protocol 3	CD31–PE CD90–PE610 Sca-1–PeCy5
Protocol 4 Isotype controls	IgG1–FITC IgG2a–PE

[†]This panel can be used to analyze either GFP^+ cells or GFP^- cells utilizing the FL 1 (488/530 nm) to evaluate the GFP-expressing populations [13]
[a]Intracellular markers that require fixation and permeabilization protocol

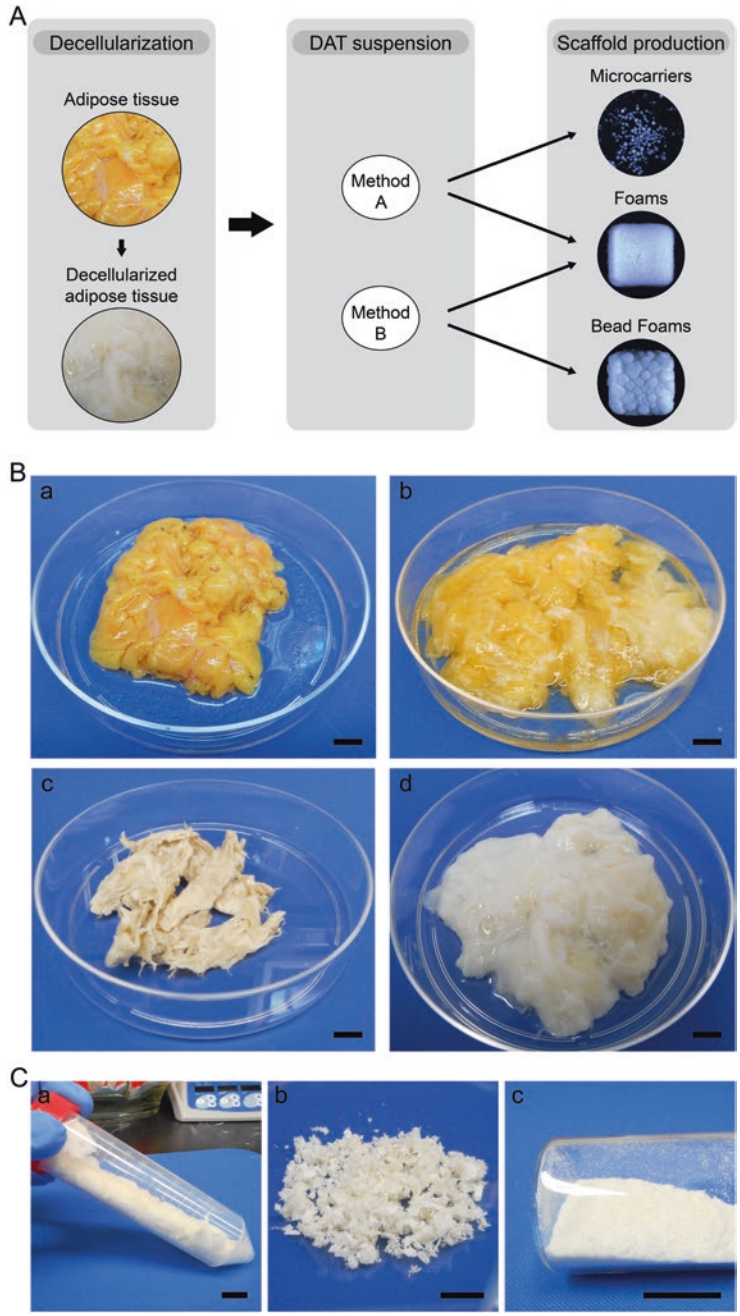

Fig. 1 Overview of adipose decellularization and further processing steps for DAT suspension preparation. (**A**) Flow chart highlighting the key stages for producing the various DAT scaffold formats. (**B**) Macroscopic tissue appearance during decellularization. (**a**) Excised adipose tissue prior to decellularization. (**b**) Tissue following the first polar solvent extraction. (**c**) Tissue after lipid extraction by mechanical pressing. (**d**) DAT hydrated in PBS. (**C**) Representative images of the DAT during further processing steps. (**a**) Lyophilized DAT. (**b**) Minced lyophilized DAT. (**c**) Cryo-milled DAT. Scale bars represent 1 cm

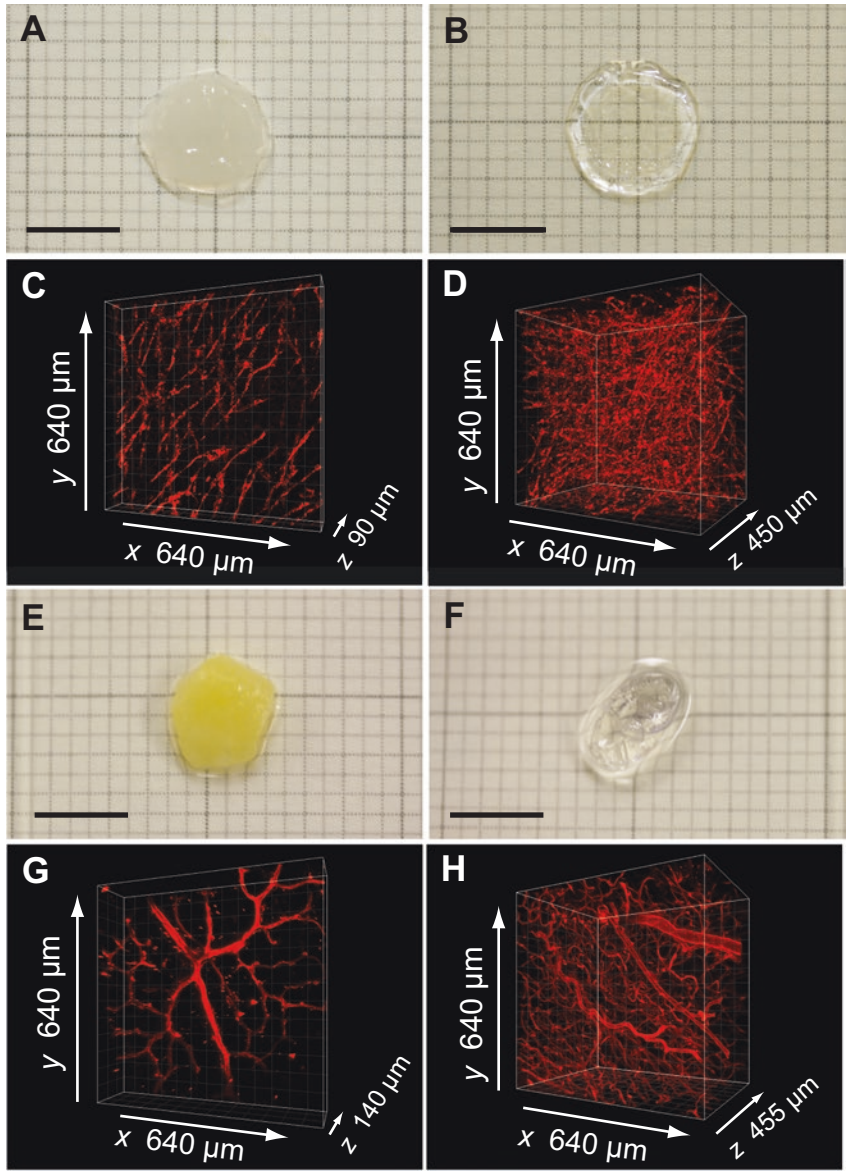

Fig. 3 Impact of optical clearing on adipose tissue samples. Tissues that were (**a**, **c**, **e**, **g**) untreated or (**b**, **d**, **f**, **h**) optically cleared illustrate the treatment's impact on the transparency of the tissue. Macroscopic appearance of samples from (**a**, **b**) an in vitro prevascularized reconstructed adipose tissue and (**e**, **f**) native adipose tissue. Bars = 5 mm. (**c** and **d**, **g** and **h**) Detection of CD31-labeled vascular structures and confocal imaging on optically cleared samples enabled to scan deeper into (**d**) reconstructed and (**h**) native adipose tissues compared to their respective untreated samples counterparts (**c**, **g**)

8. Methyl salicylate gradients (33, 66, and 100%): For a 33% solution, mix one part of methyl salicylate with two parts of methanol. For a 66% solution, mix two parts of methyl salicylate with one part of methanol.
9. Cover glasses: 24 mm × 55 mm × 0.17 mm.

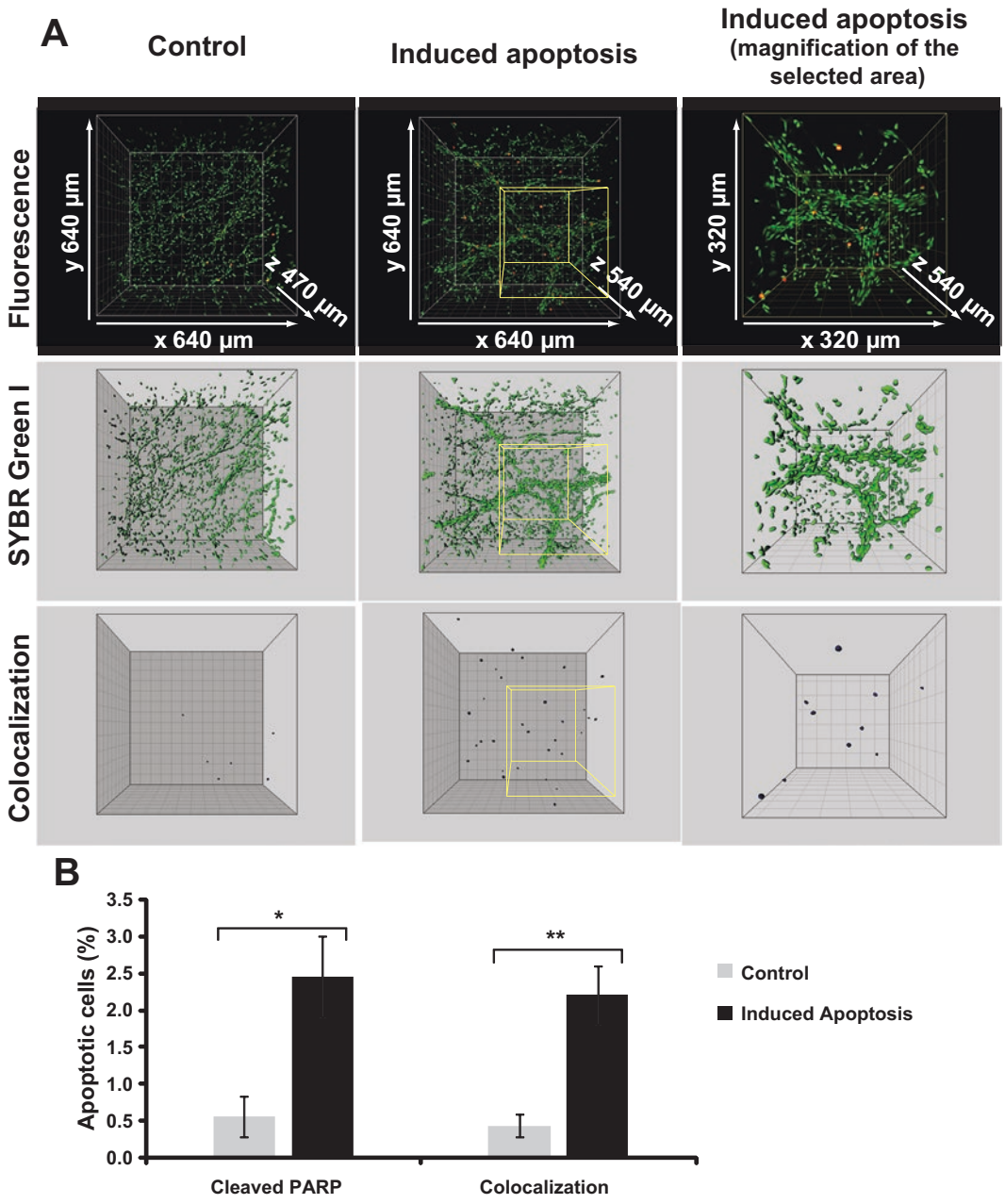

Fig. 5 Quantification of apoptotic cells by confocal microscopy on fixed tissue samples. (**a**) The quantification of apoptotic cells was performed for vehicle-treated adipose tissue explants (left column) and for staurosporine-treated samples (middle column). Higher magnifications of the selected areas are shown in the far right column. Cell detection was performed by double-labeling (top row) of cleaved PARP (apoptotic cells, in red) and SYBR® Green I (total nuclei, in green). The middle row represents Imaris-generated isosurface reconstructions from total nuclei images, while the bottom row indicates the colocalization of cleaved PARP expressing cells with SYBR® Green I positive nuclei. (**b**) Quantification of endogenous and induced apoptosis from the 3D image renderings ($n = 4$ per group, $^{*}P = 0.0037$, $^{**}P = 0.0007$, Student's *t*-tests)

3.5.7 Assessment of Multinucleation

1. Observe samples costained with Phalloidin-TRITC and DAPI under fluorescence microscope and take multiple representative images.
2. Observe areas where multiple nuclei are observed within a continuous cytoskeleton. *See* Fig. 3a for a sample image.
3. Count nuclei within the continuous cytoskeleton. Count at least six samples and six different areas from each sample and calculate the mean nuclei/cell number.

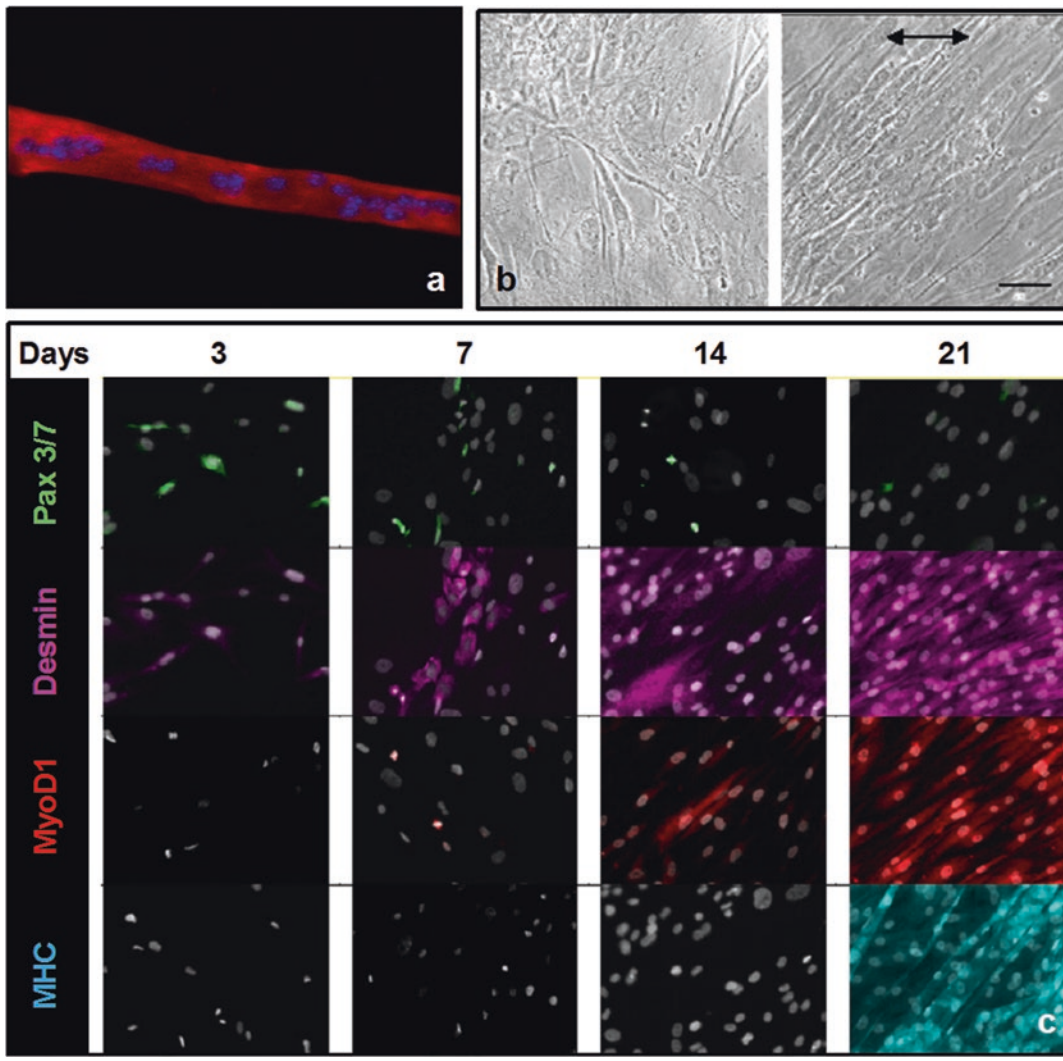

Fig. 3 Representative images of ASC myogenesis. (**a**) Multinucleation is assessed by counting the nuclei within the continuous cytoskeleton from samples costained with Phalloidin-TRITC and DAPI. (**b**) ASCs align ~45º with respect to the direction of strain (right image) (bidirectional arrow indicate the direction of strain) as compared to random cytoskeletal organization in case of static culture (left image) on Day 21. Scale bar: 50 μm. (**c**) Representative images of immunofluorescence staining for Pax 3/7, desmin, myoD, and myosin heavy chain on days 3, 7, 14, and 21 for dynamic culture conditions. ASCs were positive for desmin, myoD, and myosin heavy chain on day 21

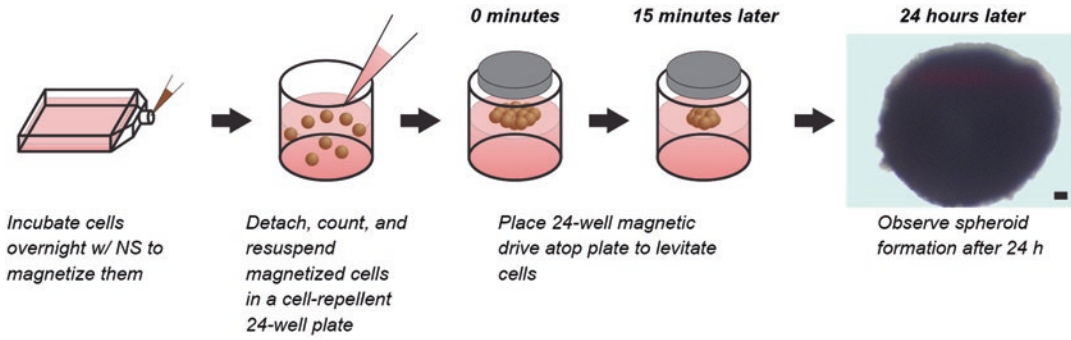

Fig. 1 Schematic of magnetic levitation of preadipocytes. Shown is a spheroid of 3T3-L1 preadipocytes in levitation. Scale bar = 100 μm

leukocytes [1]. This interest is rooted in not only the desire for a better understanding of ASC biology and growth, but also its promise as a deliverable therapeutic in it of itself as part of lipotransfer for cosmetic and functional tissue repair [6–8], as well as the numerous links between obesity and various diseases [9].

However important a research topic WAT has become, in vitro analysis of its many cellular components has proven difficult and limited its study. Traditionally, cells isolated from primary WAT would be seeded in two-dimensional (2D) monolayers on stiff plastic or glass substrates. These models do not represent native tissue environments, as they: lack a three-dimensional (3D) structure seen in vivo [10]; use rigid substrates that are much stiffer than native tissue [11–13]; have a uniform biochemical concentration gradient that is rarely seen in vivo [14]; and lack an extracellular matrix (ECM) and the accompanying cell-ECM interactions that drive tissue morphology and function [15–17]. More specifically to WAT, cells from the stromal vascular fraction (SVF), which includes ASCs, endothelial cells, and leukocytes, lose their heterogeneity when cultured together in 2D, as a result of its attachment to plastic and the domination of its mesenchymal fraction over time [18–20]. An ideal cell culture platform would replicate the 3D structure, phenotypic heterogeneity, and functionality of WAT.

Towards that end, we developed a tissue culture model of WAT using magnetic levitation (Fig. 1). The basis of magnetic levitation is the attachment of a magnetic nanoparticle assembly to cells to magnetize them and aggregate them using magnetic forces [21]. These nanoshuttles (NS), consisting of gold, iron oxide, and poly-L-lysine, work by electrostatically attaching to cell membranes, thereby magnetizing the cell. When resuspended in media, these cells can then be levitated off of any stiff substrate by placing a magnet above the culture vessel to aggregate cells towards the air liquid interface, where the cells will work with each other to build a larger 3D structure subsequently reinforced with ECM [21, 22].

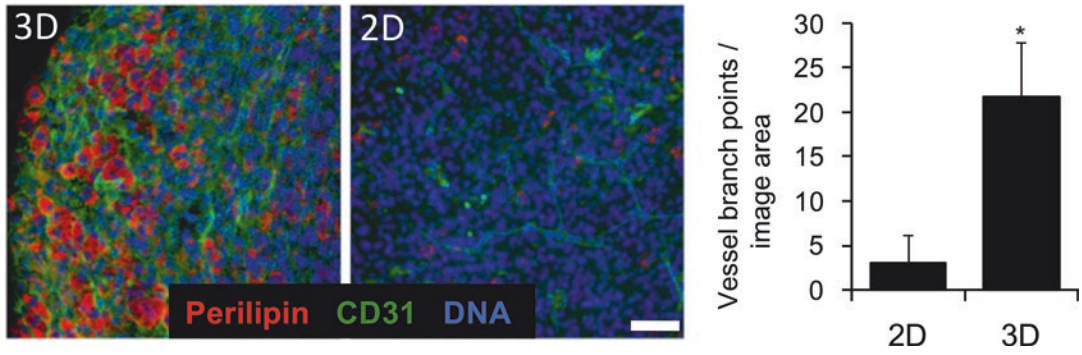

Fig. 3 Immunofluorescent stains of SVF cocultures in 3D (left) and in 2D (center) for CD31 (green) and perilipin (red). Nuclei are counterstained with DAPI (blue). SVF cells in 3D formed more vessel branch points than they did in 2D (right), supporting the idea that 3D environments promote vascularization. Scale bar = 50 μm and $*=p<0.05$

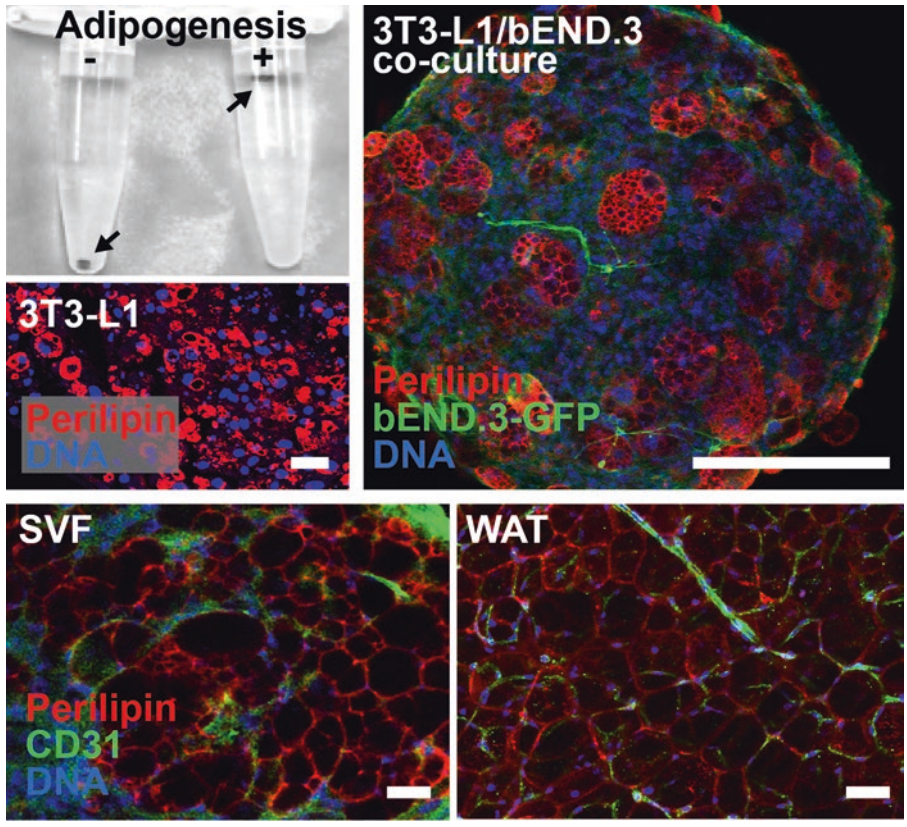

Fig. 4 Adipogenesis induction. Top left: Lipid droplet accumulation in differentiated 3T3-L1 preadipocytes is revealed from the buoyancy of the spheroid. Middle left: Positive immunofluorescent stains demonstrates lipid droplet accumulation. Top right: Adiposperes of 3T3-L1s and bEND.3 (top right) are also rich in perilipin and contain endothelial structures, demonstrating simultaneous lipogenesis and vascularization Bottom left: SVF adipospheres feature lipid accumulation and vascularization comparable to those of native mouse WAT (bottom right). Scale bar = 100 μm. Adapted from Daquinag et al. [32]

10. Quadrant analysis is performed on the fluorescence dotplot to quantify the percentage of live, necrotic, and apoptotic cell populations [36–38, 91]. The fluorescent dotplots show three cell populations: live (annexin V-FITC-negative and PI-negative; annexin V^- and PI^-) necrotic (annexin V-FITC-positive and PI-positive; annexin V^+ and PI^+), and apoptotic (annexin V-FITC-positive and PI-negative; annexin V^+ and PI^-). The quadrants positions are placed according to the no-treatment control and 5 mM H_2O_2 necrotic control (Fig. 2).

3.3.2 Adipogenesis

1. Confluent cultures of ASCs are induced to adipogenesis by replacing the medium with an adipocyte induction cocktail (*see* Subheading 2, **item 5**).
2. After 72 h, the adipocyte induction medium is replaced with adipocyte maintenance media, which contains the same components as the induction medium except IBMX and rosiglitazone.
3. Induced cells are maintained in culture for 9 days, with adipocyte maintenance medium replacement every 3 days. Upon the

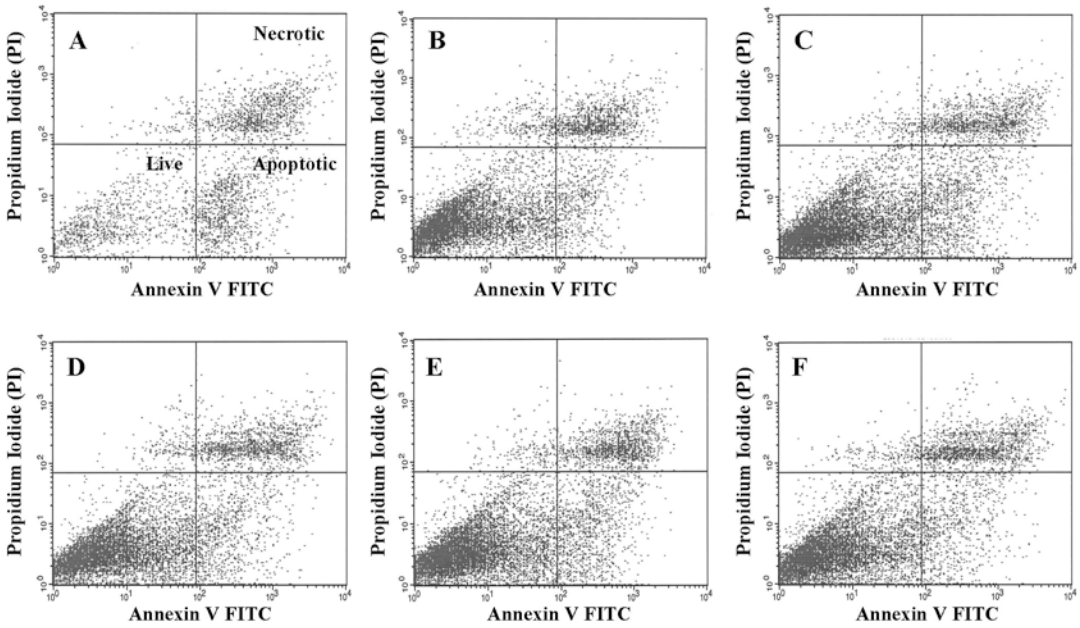

Fig. 2 Characteristic flow cytometer fluorescence dotplots showing fluorescence-activated cell sorting (FACS) analysis of SVF cells frozen/thawed in the presence various concentrations (0, 2, 4, 6, 8, or 10%) of DMSO in DMEM. Corresponding plots for other media and P1 ASCs are available in the literature [36, 38]. (**a**–**f**) represent 0%, 2%, 4%, 6%, 8% or 10% DMSO in DMEM, respectively. The fluorescent dotplots show three cell populations: live (annexin V-FITC-negative and PI-negative; annexin V^- and PI^-) necrotic (annexin V-FITC-positive and PI-positive; annexin V^+ and PI^+), and apoptotic (annexin V-FITC-positive and PI-negative; annexin V^+ and PI^-). The quadrants positions were placed according to the no-treatment control, 40 μm etoposide apoptotic control, and 5 mM H_2O_2 necrotic control. Reprinted with permission from [37]

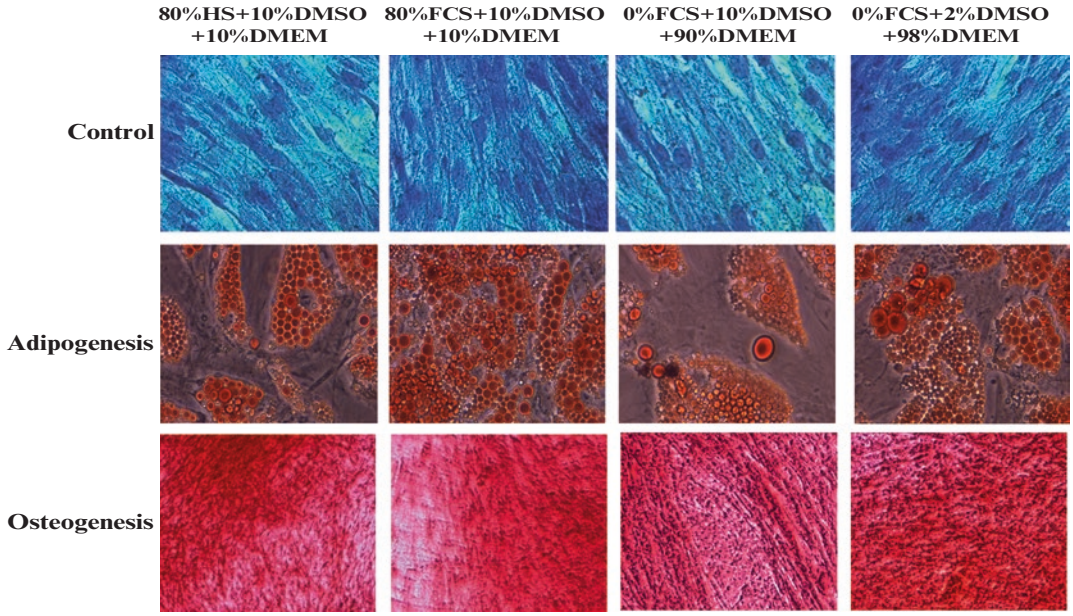

Fig. 3 Representative phase contrast photomicrographs of P1 ASCs cultured under untreated (first row; Toluidine Blue staining), adipogenic (second row; Oil Red O staining), or osteogenic (third row; Alizarin Red staining) conditions. Corresponding plots for other media and SVF cells are available in the literature [37, 38]. Adipogenic cultures were stained with Oil Red O 14 days after induction, while osteogenic cultures were stained with Alizarin Red after 21 days of culture. Images in column 1 represent cells that were cryopreserved in media containing 80% FCS with 10% DMSO in DMEM. Images in column 2 represent cells that were cryopreserved in media containing 80% HS with 10% DMSO in DMEM. Images in column 3 represent cells that were cryopreserved in media containing 0% FCS with 10% DMSO in DMEM. And finally, images in column 4 represent cells that were cryopreserved in media containing 0% FCS with 2% DMSO in DMEM. Reprinted from [36]

ninth day, the cultures are washed twice with prewarmed PBS and fixed in formalin at 4°C. Adipocyte quantification is determined by staining neutral lipids with Oil Red O (Fig. 3).

3.3.3 Osteogenesis

1. Confluent cultures of ASCs are induced to osteogenesis by replacing the medium with an osteogenic induction cocktail (*see* Subheading 2, **item 6**).
2. The induced cells are fed fresh osteogenic induction media every 3 days for 3 weeks. The cultures are then washed with 0.9% sodium chloride solution and fixed in 70% ethanol.
3. Osteoblast quantification is determined by Alizarin Red staining for calcium phosphate (Fig. 3).

3.4 Some Observations on the Effect of Various Cryoprotectants on the Post-freeze–Thaw Response of SVF of Adipose Tissue

1. The data suggests that the choice of the serum (human serum, HS; or fetal calf serum, FCS) does not significantly alter the SVF cell survival when frozen/thawed in 10% DMSO and DMEM.
2. The highest % of postthaw survival is achieved with a concentration of 8% DMSO (~73%), the postthaw survival values obtained with DMSO concentrations of 2, 4, 6, and 10% are comparable and are ~60%, ~63%, ~66%, and ~70%, respectively.

Fig. 3 Transplantation of ASCs–PRP admixture. ASCs–PRP admixture was transplanted into the calvarial defect. Then the periosteum and skin flaps were placed back using 6-0 sutures

3.8 Calvarial Bone Dissection

1. Euthanize rat with an overdose of intraperitoneal injection of pentobarbital sodium.
2. Place the rat in the prone position and inject the xylocaine (0.5 mL of 1%) intradermally in the middle of the calvarium.
3. Make a midline calvarial incision and elevate the cranial skin flaps. Divide the subcutaneous fascia and remove the calvarial bone using a straight fissure bur with a micromotor.

3.9 Tissue Preparation and Micro-Computed Tomography (CT) Analysis

1. Specimens are fixed in 4% paraformaldehyde (PFA), after which Micro-CT was performed.
2. The surface area and volume of newly formed bone in the defect site are calculated using Analysis software (Fig. 4, *see* **Note 2**). A representative image of Micro-CT is shown in Fig. 5.

3.10 Fixation, Decalcification, and Histological Analysis

1. Fix in 4% paraformaldehyde solution for 7 days at room temperature.
2. Decalcify the specimens using decalcification solution for 2–3 days (*see* **Note 3**).
3. Cut the specimens at the center of calvarial bone using surgical blade.
4. Wash the specimens with water and then embed them in paraffin.